



Formation of Glasses from Liquids and Biopolymers

Author(s): C. A. Angell

Source: *Science*, New Series, Vol. 267, No. 5206 (Mar. 31, 1995), pp. 1924-1935

Published by: American Association for the Advancement of Science

Stable URL: <http://www.jstor.org/stable/2886440>

Accessed: 18/09/2008 09:14

Your use of the JSTOR archive indicates your acceptance of JSTOR's Terms and Conditions of Use, available at <http://www.jstor.org/page/info/about/policies/terms.jsp>. JSTOR's Terms and Conditions of Use provides, in part, that unless you have obtained prior permission, you may not download an entire issue of a journal or multiple copies of articles, and you may use content in the JSTOR archive only for your personal, non-commercial use.

Please contact the publisher regarding any further use of this work. Publisher contact information may be obtained at <http://www.jstor.org/action/showPublisher?publisherCode=aaas>.

Each copy of any part of a JSTOR transmission must contain the same copyright notice that appears on the screen or printed page of such transmission.

JSTOR is a not-for-profit organization founded in 1995 to build trusted digital archives for scholarship. We work with the scholarly community to preserve their work and the materials they rely upon, and to build a common research platform that promotes the discovery and use of these resources. For more information about JSTOR, please contact support@jstor.org.



American Association for the Advancement of Science is collaborating with JSTOR to digitize, preserve and extend access to *Science*.

Formation of Glasses from Liquids and Biopolymers

C. A. Angell

Glasses can be formed by many routes. In some cases, distinct polymorphic forms are found. The normal mode of glass formation is cooling of a viscous liquid. Liquid behavior during cooling is classified between "strong" and "fragile," and the three canonical characteristics of relaxing liquids are correlated through the fragility. Strong liquids become fragile liquids on compression. In some cases, such conversions occur during cooling by a weak first-order transition. This behavior can be related to the polymorphism in a glass state through a recent simple modification of the van der Waals model for tetrahedrally bonded liquids. The sudden loss of some liquid degrees of freedom through such first-order transitions is suggestive of the polymorphic transition between native and denatured hydrated proteins, which can be interpreted as single-chain glass-forming polymers plasticized by water and cross-linked by hydrogen bonds. The onset of a sharp change in $d\langle r^2 \rangle/dT$ ($\langle r^2 \rangle$ is the Debye-Waller factor and T is temperature) in proteins, which is controversially identified with the glass transition in liquids, is shown to be general for glass formers and observable in computer simulations of strong and fragile ionic liquids, where it proves to be close to the experimental glass transition temperature. The latter may originate in strong anharmonicity in modes ("bosons"), which permits the system to access multiple minima of its configuration space. These modes, the Kauzmann temperature T_K , and the fragility of the liquid, may thus be connected.

Glass, in the popular and basically correct conception, is a liquid that has lost its ability to flow. Thus, instead of "taking the shape of its container," it can itself serve as the container for liquids. Yet structurally a glass is barely distinguishable from the fluid substance it was before it passed, quite abruptly in some cases, into the glassy state. What is going on? Why did this particular substance or solution suddenly undergo this dramatic "slowing down" in the diffusive motions of its particles? Why do glasses not form a precisely ordered crystalline material, at some precisely defined freezing point, like so many other, more "normal," substances? These questions, once the domain of ceramists and polymer scientists, are now being addressed by physicists as well as materials scientists. This article presents an overview of their many fascinating aspects and highlights some of the surprises that have turned up recently in efforts to answer these questions.

The answers to these questions impact on a wide range of disciplines. Everyone knows the central importance of the glassy state to the optical sciences (and has some awareness of the role of thermal history and slow relaxation in determining refractive index stability and other properties), but it has only been recently recognized that it is the glass transition and the associated diffusive slowdown that plays a central role in the preservation of food and suspension of desert insect life during drought. That most polymers in everyday use are noncrystalline

solids is general knowledge, but that rubber bands splinter like dropped goblets when impacted at liquid nitrogen temperature usually comes as a surprise. And while it is common knowledge that glass occurs naturally (volcanic glass provided material for native American arrowheads), the idea that most of the universe's water exists in the glassy state (in comets, formed by condensation from the gaseous state at very low temperatures) is a recent one.

The last mentioned instance, naturally occurring glassy water, shows that glasses are not necessarily formed by the cooling of an initially liquid state. Indeed, the glassy state can be obtained by many different routes and yet appear to be fundamentally the same substance. Vitreous silica, the archetypal (although atypical) glass material, can be obtained by the cooling of liquid silica, by vapor condensation (the manner

in which the silica mirror base of the Mount Palomar telescope was fabricated), by heavy particle bombardment of a crystalline form, by chemical reaction (hydrolysis) of organosilicon compounds followed by drying, and by vapor-phase reaction of gaseous molecules followed by condensation. Indeed only the latter route, (with the use of highly purified reactants) produces glass of purity sufficient for the demands of the fiber optics communications technology. Although the densities of the products of these very different processes may not be identical without annealing procedures, it would take an expert to tell them apart on the basis of their x-ray diffraction patterns. The different routes for preparing glasses are summarized in Fig. 1 (1).

For many substances and mixtures of substances, there are noncrystalline packing modes for the atoms and molecules that are of intrinsically low energy and into which these particles can easily assemble. These may not be the lowest energy packing modes (most negative relative to the vapor), as is demonstrated by the release of heat when crystallization occurs, but they are sufficiently low that the stabilization associated with the large number of alternative packings with the same or similar energy, makes their occurrence as a state of matter very probable when the time available for finding a condensed state is a factor. For the so-called "good glass formers," the probability of germinating a crystal rather than forming a glassy solid during cooling at normal rates is so small that crystals simply do not form. In the case of liquid B_2O_3 (a key ingredient of Pyrex glass) at ambient pressure, crystals do not grow even when the melt is seeded with a crystallite of the stable phase because the driv-

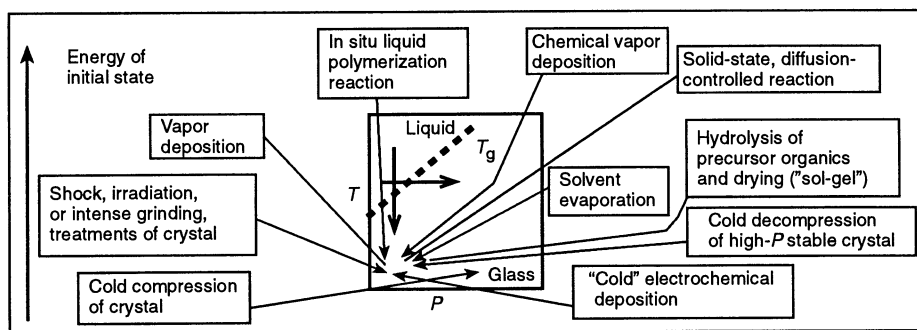


Fig. 1. Various routes to the glassy state, roughly indicating the energies of the initial states relative to the final glassy states. The route of crystal compression below T_g may yield glasses that are thermodynamically distinct from those obtained by the other routes but which may transform to them by way of nonequilibrium first-order transitions.

The author is in the Department of Chemistry, Arizona State University, Tempe, AZ 85287-1604, USA.

ing force is so small and the kinetics are so slow. Crystallization in this case can only be induced by raising the pressure (2). In certain binary solutions at low temperatures, the glassy state appears to be thermodynamically stable with respect to any combination of crystals or crystal plus solution (3).

This article reviews some of the key aspects of the phenomenology of glasses as they form by the conventional and most thoroughly studied route, the cooling of a liquid with concomitant diffusive slowdown. These observations are then applied to many other glass-forming systems, including proteins and other biopolymers (4, 5). In the latter one finds as a common occurrence, the possibility of multiple glasses—at least of glassy states with very different packings of their constituent particles, for instance coils or helices or, with some provisos, native versus denatured structures. Although recognized as a possibility long ago (6), such polymorphism (7) in inorganic systems was properly demonstrated only in 1984 (8, 9) when the possibility of vitrifying H₂O by compression of ice crystals was announced. This process revealed a dense vitreous phase that transformed suddenly to the familiar low-density amorphous solid water on decompression and annealing. These new developments will be reviewed after the groundwork of the subject has been laid out.

Glass Formation by Diffusive Slowdown

Separation of characteristic time scales. If crystals do not form during cooling (see below), then the glassy state is entered when the cooling liquid passes through the “glass transition,” which is actually a range of temperatures over which the system “falls out of equilibrium.” The range is that needed to change the average relaxation time (a quantity to be discussed in more detail below) by some two to three orders of magnitude, usually between 10² s and 0.1 s (10, 11). It is manifested most directly by a rapid decrease of heat capacity C_p from liquidlike to crystal-like values as the liquid degrees of freedom become kinetically inaccessible. This abrupt decrease in the C_p (usually between 40 and 100% of the vibrational C_p) and the corresponding increase on reheating, is regarded by most workers as the primary signature of the transition between ergodic and nonergodic states [ergodicity breaking (12)]. The glass transition temperature T_g , per se, is usually defined as the temperature of onset of the C_p increase ΔC_p during heating, usually at 10 K/min (the definition of T_g is always arbitrary, and there is no international convention on the subject). It is illustrated in Fig. 2 for some extreme cases where crystal, glass, and liq-

uid state C_p 's are compared.

A visual picture of atomic-level motions can be gleaned from one of the simplest of all glass-forming systems, one which has become a model system for many of the sophisticated experimental studies that have been performed to test the predictions of the mode-coupling theory (MCT) of viscous slowdown (13–15). This is the binary ionic liquid consisting of two cations with the same electronic structure as argon (K⁺ and Ca²⁺) and a simple triangular anion NO₃⁻ which occupies about the same volume as the chloride ion (which is also isoelectronic with argon). It may be formed by melting the anhydrous salts KNO₃ and Ca(NO₃)₂ in the molar proportions 3:2 (16). Nicknamed CKN, this melt has been the subject of most of the physical measurements that can usefully be made in the attempt to understand liquid and glass behavior.

At high temperatures, CKN can be visualized as an enormous collection of tiny charged particles that are in a state of ceaseless violent motion. Chaotic trajectories constantly bring particles into collision with neighboring particles (of opposite charge type). On average, the collisions simply cause a reversal in the trajectories of the ions, so they appear to be rattling, but sometimes a change of relative positions occurs by an ion glancing past its immediate neighbors into transient voids or channels, which quickly become new centers of rattling. In the highly fluid state typical of

liquids near their boiling points, the latter (diffusive) motions occur frequently; computer simulation studies of liquids would suggest a rate of once for every 10 trajectory reversals. The distinction between rattling and diffusing motions will necessarily be blurred under these conditions, and it would be reasonable to say that the particles are undergoing continuous diffusion (“itinerant oscillators”).

As temperature decreases and, correspondingly, the volume occupied by the ions decreases (liquids expand more rapidly than glasses or crystals), the average particle spends an increasing fraction of the time in trajectory-reversing collisions with its neighbors because the conditions needed for a diffusive displacement to occur become more stringent. With less volume available, more cooperation is needed between neighbors in order for one to escape its initial cage and the time taken for a given particle to diffuse one interionic distance increases; this is (17) approximately the “structural relaxation time” obtained by various measurements to be referred to below. Meanwhile, the time between trajectory reversals remains constant. On the occasions when a particle does undergo a diffusive motion—one which relocates its center of vibration with respect to those of some of its neighbors—more cooperation is involved. There is some evidence from computer simulations of spin system analogs (18), supported by theory (19), that the motions which permit diffusion to occur take place preferentially or exclusively within “loose” or mobile regions of the structure—regions that may become of nanoscopic dimensions near T_g (20–22).

Whatever the details, however, the essential feature of vitrification is that, as T_g is approached, an enormous gap opens up between the time for trajectory reversal (the “rattling time”) and the time for structural equilibration (relaxation time). The difference in these two time scales can change by as much as 10 orders of magnitude in the temperature range T_g to 1.1 T_g (although it may also be much more gradual, as discussed below). Through all this C_p remains unaffected until the transformation range is entered. The transformation range involves the last two to three orders of magnitude before T_g is reached, so it can be a quite sharply defined phenomenon. At the T_g defined as in Fig. 2, the relaxation time proves to be ~100 s (10), 17 orders of magnitude longer than the rattling time. When the liquid can only relax stress, that is, behave like a liquid, on the time scale of hours, then experiments with characteristic time scales of minutes, like scanning calorimetry, will only see the unrelaxed, nondiffusive (solid-like) aspect of the substance. Consequently, C_p decreases to crystal-like values

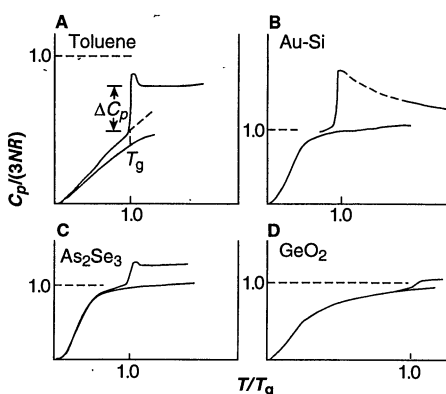


Fig. 2. Heat capacity forms for liquid and crystal phases of different substances. (A) Molecular systems like toluene where the glass transition occurs over a range where the crystal heat capacity is not classical; (B) metallic systems like Au-Si where crystal and glass reach the classical regime before the glass transition occurs; (C) covalent systems like As₂Se₃ where the jump in liquid heat capacity occurs on a classical background and ΔC_p remains large above T_g ; (D) open network systems like GeO₂ where ΔC_p is small and occurs on a classical background. The T_g is usually defined by the construction made at 10 K/min shown in (A) because this fixes T_g as the temperature where the average structural relaxation time is 100 s (10) for scanning at 10 K/s; N is the number of atoms per formula unit and R is the gas constant.

when measured during cooling, with a corresponding somewhat sharper increase on reheating.

For the increasingly popular computer simulation studies of supercooling liquids, the loss of ergodicity perforce occurs in a completely different, much shorter, time scale range, and this causes the "transition" to become a much less well-defined phenomenon (11, 23). In this case T_g , when it is defined at all, is usually taken as the intersection of lines drawn through values of system energy, or volume, obtained for temperatures well above and well below the ergodicity-breaking regime which now extends over a range of T comparable with the value of T_g itself (23–25). The value of T_g now falls at relaxation times much closer to the rattling time, and depends very much on the available computer time. The limitations set by computation speeds is a serious problem for stimulation studies, which can only explore a modest range of viscosities. A great advantage of such studies, on the other hand, is the improbability of crystallization in all but the very simplest liquids (hard spheres and inert gases): It simply never has time to happen (26).

Beating the crystallization trap. To workers in the field of supercooled liquids and glass formation, crystallization is an experimental disaster to be avoided wherever possible. Except in rare cases (like the B_2O_3 mentioned earlier, and a few silicate glasses) once a "critical nucleus" has formed by some chance fluctuation, crystallization is inevitable and is often catastrophic to apparatus. The nucleation event, in which a small but critical number of unit cells of the stable phase self-assemble, is one that either involves many more particles than are involved in the cooperative rearrangement needed for the structural relaxation, or involves a less probable fluctuation of a similar number. This is because, in all recognized glass-forming systems, it has a much longer time scale than the relaxation time (τ_{in}).

It is useful to define an escape time τ_{out} (27), which is the time necessary to convert ~50% of the liquid to crystalline material by a process of nucleation and crystal growth. The probability (per unit time and volume) of the occurrence of a nucleation event usually passes through a maximum during cooling between T_m and T_g (28, 29) and so τ_{out} exhibits a minimum. For safe experiments, it is necessary to choose systems, or compositions within systems, in which this minimum nucleation time remains long compared with the time scale for preparing the system for the experiment (The reader can be forgiven for protesting that at this point four distinct time scales, one for rattling, one for relaxing, one for crystallizing, and one for setting up the experiment, must be juggled.). "Good glass

formers" are those with very low nucleation probabilities at all temperatures. They usually show no maximum nucleation rate, or at least none above T_g . For poorer glass formers, a "critical cooling rate" (29) needs to be exceeded.

The nucleation probability can be determined experimentally (30) and has been intensively studied. An excellent review is that of James (31). Crystallization usually involves more than just nucleation. A separate factor is the growth rate of nuclei, which always increases with increasing temperatures except near the liquidus (25). The maximum crystallization rate is found at temperatures somewhat above the temperature of maximum nucleation rate and is easily determined by isothermal calorimetry studies (32).

For molecular liquids, the likelihood that crystallization can be avoided during cooling at easily achieved rates (such as by quenching a small test tube of the test liquid by dipping it in a liquid nitrogen bath) can be predicted empirically by the $T_v/T_m > 2$ rule. Liquids with melting points less than half their vaporization points are usually sufficiently viscous at their melting points that the nucleation rate during quenching to lower temperatures is insufficient for crystallization to occur. The physics behind this empiricism has been discussed (29, 33, 34).

Strong and fragile liquids, and systems that can be both. Notwithstanding the arguments for an underlying phase transition (35), it is generally agreed that the process called the glass transition, as actually observed in the laboratory during cooling, is strictly kinetic in origin. Indeed what is observed is just what is to be expected when an internal relaxation time, one intrinsic to the liquid,

crosses an experimental time scale. To understand the glass transition as a general phenomenon it must first be understood how this internal relaxation time, which is proportional to the viscosity, changes with T .

Viscosity data for ionic and molecular substances are assembled in Fig. 3, which by itself offers little basis for generalization. However, if the available data are scaled according to some simple principle, improvements in comprehensibility result. The most common scaling temperature, namely, by the gas-liquid critical temperature, is not useful because of lack of data and other considerations. However, a natural choice that lies at the other end of the viscosity range, namely, T_g (defined in a reproducible way), leads to Fig. 4 (17, 36).

Figure 4 is based on the choice of an invariant viscosity at the scaling temperature T_g (10^{13} poise at the glass transition), and the diagram thus produced (36) has been accorded a lot of attention. However, the choice of $T_{(\log \eta = 13)}$ as the scaling temperature is not necessarily the best choice. Alternatives based on (i) T_g defined by scanning calorimetry at a standard rate and (ii) the temperature at which certain relaxation times reach 10^2 s, have also been utilized (17, 34). Although the patterns obtained according to such choices differ in some detail, the broad aspect is unchanged. The almost universal departure from the familiar Arrhenius law is perhaps the most important canonical feature of glass-forming liquids. Two others will be discussed below.

Figure 4 suggests that certain types of liquids form extremes on the general behavior. Open network liquids like SiO_2 and GeO_2 show an Arrhenius variation of the viscosity (or structural relaxation time) be-

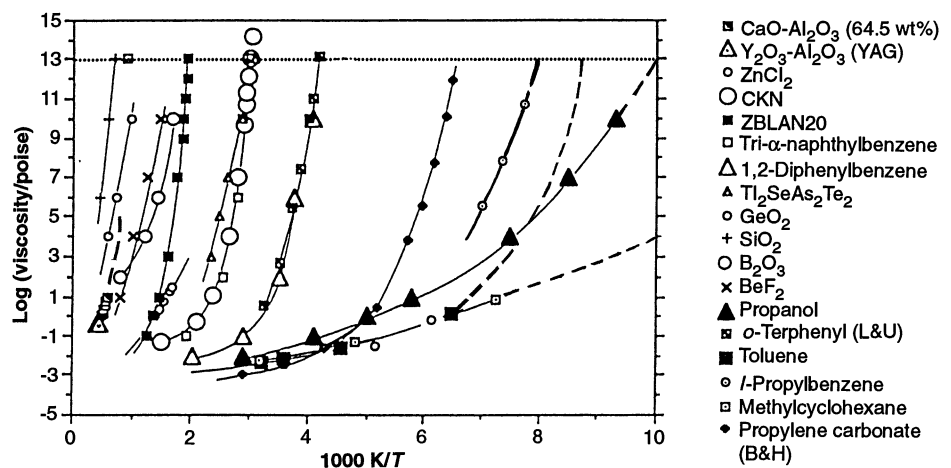


Fig. 3. Variations of the viscosity with temperature, plotted in Arrhenius form, for a variety of liquids of different types with different calorimetric glass transition temperatures. The T_g value is roughly the temperature at which the viscosity reaches 10^{13} P except for fragile molecular liquids, where T_g falls at viscosities up to four orders of magnitude lower. Dashed lines are interpolations between T_g and the lowest temperature data point. Source of data are given in earlier publications (17, 36, 59) and are indicated here by authors' initials; ZBLAN20, $[ZrF_{4.053}[BaF_{2.0,20}[LaF_{3.0,04}[AlF_{3.0,03}[NaF]_{0.20}]_0.20]$.

tween T_g and the high-temperature limit and provide the "strong" liquid extreme of the pattern. Others, characterized by simple nondirectional coulomb attractions or by van der Waals interactions in a subgroup of substances with many π electrons (primarily aromatic substances), provide the other extreme, "fragile" liquids. In fragile liquids, the viscosities vary in a strongly non-Arrhenius fashion between the high and low limits. This strong/fragile liquids pattern (17, 36) has become has been used as the basis for a classification of liquids, to indicate the sensitivity of the liquid structure to temperature changes. Fragile liquids have glassy state structures that teeter on the brink of a collapse at their T_g 's and which, with little provocation from thermal excitation, reorganize to structures that fluctuate over a wide variety of different particle orientations and coordination states. Strong liquids, on the other hand, have a built-in resistance to structural change, and their vibrational spectra and radial distribution functions show little reorganization despite wide variations of temperature. Strong liquids can be converted to more fragile behavior by changing their densities—an example will be given below. Strong liquids typically show very small jumps in ΔC_p at T_g , whereas fragile liquids show large jumps. This contrast is indicated by the insert in Fig. 4. Hydrogen bonding seems to make a

special contribution to ΔC_p .

The whole pattern can be reproduced quite well by variation of one parameter in a modified version of the famous Vogel-Fulcher or Vogel-Tammann-Fulcher (37-39) equation (40, 41). The original equation:

$$\eta = \eta_0 \exp[B/(T-T_0)] \quad (1)$$

can be written in the form:

$$\eta = \eta_0 \exp[DT_0(T-T_0)] \quad (2)$$

In this form the parameter D controls how closely the system obeys the Arrhenius law ($D = \infty$). The effect of changing D from 5 to 100 is shown in the insert to Fig. 4. As D changes, so will the value of T_0 change relative to T_g ; the relation is a simple linear one of the form

$$T_g/T_0 = 1 + D/(2.303 \log \eta_g/\eta_0) \quad (3)$$

where $\log(\eta_g/\eta_0)$ is ~ 17 (42-44), according to Fig. 4.

The most fragile liquids identified to date are polymeric in nature and cannot be entered into a figure like Fig. 4 without modification because the viscosity of a polymer liquid is largely controlled by its molecular weight. This effect must be removed before any common pattern can be obtained. It is preferable in classifying polymer liquids and rubbers to utilize some relaxation time characteristic of the segmental

motions, that is, a microscopic relaxation time, such as is obtained from transient mechanical spectroscopy near T_g , digital correlation spectroscopy, or dielectric relaxation. When this is done (45, 46), polycarbonates and polyvinyl chloride prove to be the most fragile systems yet identified with $D \sim 2$.

The equivalent treatment of magnetic relaxation in spin glasses, which have much phenomenology in common with glass-forming liquids, shows (47) that much more fragile behavior can be found in some of those systems, such as Cu-Mn. In this case Eq. 3 shows that T_g and T_0 will almost coincide, which is probably the reason for suggestions that in some spin glass systems there is a real phase transition with an associated diverging length scale.

It is to be stressed that Eq. 2 no means accurately describes the behavior of any liquid over the entire 15 orders of magnitude for which data are available, although it does remarkably well for some liquids in the middle of the Fig. 4 pattern, such as glycerol (48, 49). Generally speaking, the more fragile the liquid, the poorer the fit. Many other two and three parameter equations [summarized in (1)] have been proposed, but none perform significantly better than Eq. 2. Also, the key parameter in Eq. 2, T_0 , which best fits the data in the temperature domain entailing the last six orders of magnitude in τ before T_g (50, 51) (or the entire range for glycerol), can frequently be predicted independently by the purely thermodynamic analysis (52) described below.

On the other hand, a different picture emerges from a recent analysis of data on many fragile systems in which adherence to Eq. 2 is tested rather stringently through a differential analysis (49). This analysis, which emphasizes the shorter relaxation time data, suggests that Eq. 2 better fits data in a higher temperature domain. Fitted in this domain, the T_0 parameter no longer coincides with the Kauzmann temperature T_K (defined below). Indeed it is unphysical, lying above T_g . Thus there is little that is physically robust to be found in quantitative analysis of the relaxation-time temperature dependence.

An analysis of the higher temperature, lower viscosity data which has gained much credence in recent years is that based on the very detailed predictions of mode coupling theory, MCT (14, 15). This is described as a mathematical theory of the glass transition (15) and, as such, much of the physical picture has had to be put in a posteriori. There has been some confusion in nomenclature as a result. However, its success in detailing subtle aspects of the phenomenon in the simple atomic systems to which it might be expected to apply (53), [and also to many more complex systems to

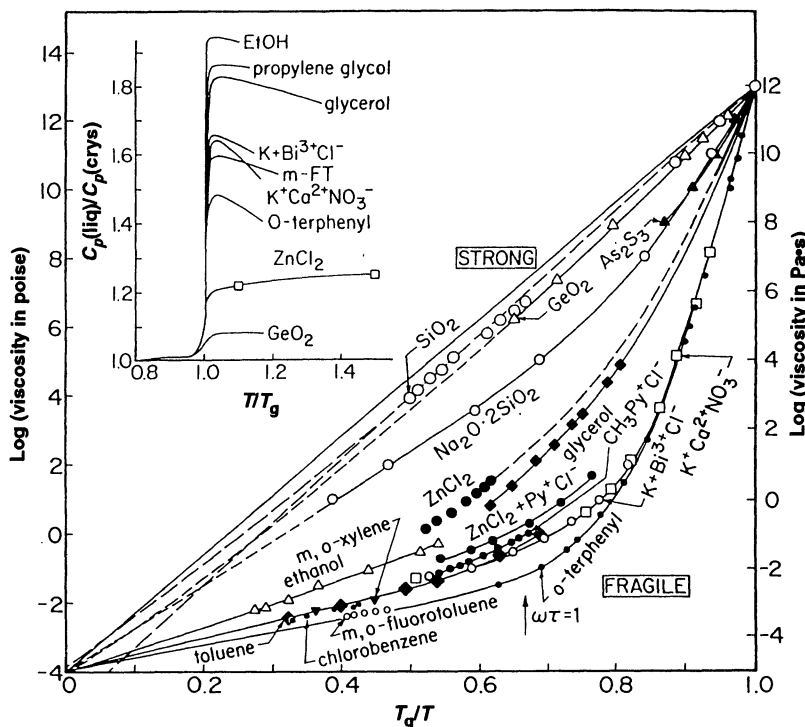


Fig. 4. Arrhenius plots of the viscosity data scaled by values of T_g from Fig. 3 and other sources showing the "strong-fragile" pattern of liquid behavior on which the liquid's classification of the same name is based. As shown in the insert, the jump in C_p at T_g is generally large for the fragile liquids and small for strong liquids, although there are a number of exceptions, particularly when hydrogen bonding is present. [From (36)]

which application is less expected (54)] is by all accounts remarkable. In this theory, at least in its more tractable versions in which activated processes play no role (14), thermodynamics has no direct role to play. The theory in its idealized version requires the liquid dynamically to jam into a glassy state at temperatures far above T_g and in some cases above T_m , while a fast relaxation mode [which bears no relation to the familiar Johari-Goldstein β -relaxation (55)] continues to be active in the glassy state. The jamming is in practice avoided by the intervention of activated processes which, for time scales longer than nanoseconds, offer an alternative and more efficient way of relaxing stress to that dealt with by the idealized theory. The "hopping" processes are incorporated in a more advanced form of the theory (15) but this form is highly parameterized and the predictive prowess in the hopping domain is less marked.

Before the onset of the activated processes, all aspects of the liquid dynamics are controlled by the structure factor. Consistent with this "single order-parameter description," the Prigogine-Defay ratio (56) (defined below), in the relaxation time range where MCT has been found accurate (namely, those cases accessible to computer simulation), is found to be unity (24).

For real systems in the temperature range approaching T_g , the Prigogine-Defay ratio always exceeds unity (57, 58). Because of the great increase in complexity that accompanies the extension of MCT into the low-temperature activated regime, MCT has had little to say about this long relaxation time domain, yet it is in this domain that technologically important processes such as refractive index stabilization, mechanical strengthening, and physical aging are important problems to be understood and controlled. In the low-temperature regime, the "fast" process of MCT, that is, the process associated with anharmonic prediffusion behavior, remains relevant because barrier crossing must also be preceded by cage rattling. However, now it is the physics of exploration of the "energy landscape," which must be dealt with in understanding the slow processes. In this sense, as pointed out before (59), MCT advances the field to the edge.

The crossover to barrier-dominated behavior was anticipated in a classical paper by Goldstein, who introduced the potential energy hypersurface to the field (60). Strength and fragility in liquids may be discussed in terms of simple two-dimensional representations of this energy hypersurface (1, 17, 59), as discussed in detail by Stillinger (61). Fragile liquids would have high densities of minima per unit energy increase, in order to account for their high configurational ΔC_p 's. They would also

need relatively low barriers between the minima. This corresponds to small D of Eq. 2 because, in the most successful model for relaxation near the glass transition (62), D of Eq. 2 is proportional to $\Delta\mu/\Delta C_{p,o}$, where $\Delta\mu$ is the height of the barrier between minima and $\Delta C_{p,o}$ is the configurational heat capacity at T_K . Surfaces with few minima and high energy barriers between minima generate strong liquids while intermediate liquids can have various origins (63).

The problem of deriving the features of the potential energy hypersurface from the basic intermolecular potentials is a formidable one (64) and the means of describing its topology in intelligible terms must be even more daunting. A useful approach is suggested by some recent observations on the archetypal strong liquid SiO_2 . Computer simulations of this system (65–68) suggest that the diffusivities behave in an anomalous fashion and increase with increasing pressure. Brawer's analysis (69) indicates that this happens because the increased density provides an increased probability of transiently or temporarily increasing the coordination number of Si from 4 to 5, permitting diffusive exchange of O between adjacent Si atoms. The same packing factor is involved in changing the liquid character from strong to fragile. It seems likely that increasing density changes both the $\Delta\mu$ and ΔC_p factors in a fragility-favoring manner. Although laboratory experiments to establish these effects are difficult, the ion dynamics simulations needed to study them are now within reach, although extremely long runs (simulating >1 ns to obtain reliable data at the lower temperatures.)

When the density of silica was raised by 30%, the diffusivities of the Si and O components changed from behavior consistent with the strong liquid of ambient pressure experience to a strongly non-Arrhenius liquid (1, 66). These results suggest a change-over from strong to fragile behavior as a

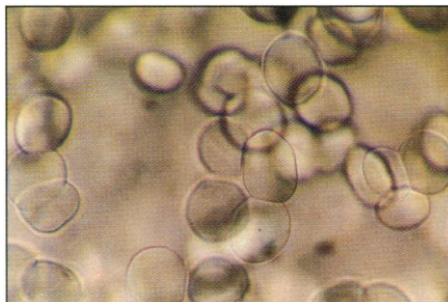


Fig. 5. Microstructure showing two glassy phases of identical composition formed by quenching an initially homogeneous oxide melt in the system $\text{Y}_2\text{O}_3\text{-Al}_2\text{O}_3$. The droplet phase has a lower density and has evidently nucleated from the denser phase, which is a fragile liquid at 2000 K (Fig. 4), during quenching. [From (70) by permission copyright Macmillan]

function of particle packing density. Thus, a given hypersurface may have different regions, corresponding to different particle densities, which have very different densities of minima (discussed further below). These results suggest that a rigid ion system like BeF_2 or SiO_2 could provide a fruitful subject for theoretical investigations of the hypersurface topologies which relate alternatively to strong and fragile behavior in liquids.

Fragile-to-strong liquid conversions by first-order transitions. What remains to be shown is that, in certain interesting cases, regions with different topologies must be character-

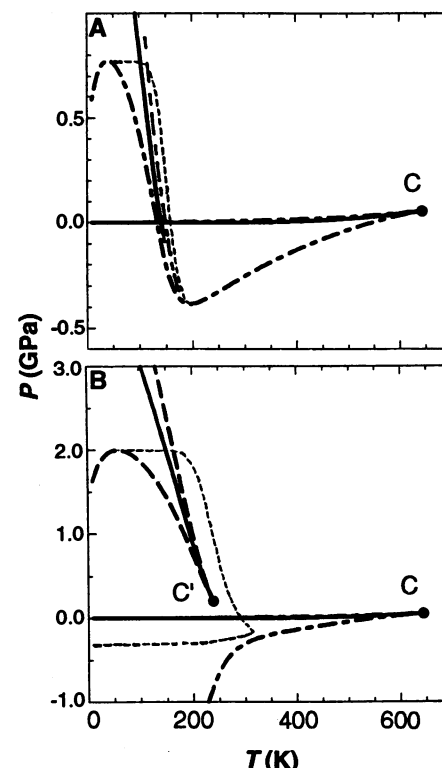


Fig. 6. Phase diagrams from modified van der Waals model for water (76) based on choice of (A) the hydrogen bond-breaking energy consistent with spectroscopic evidence (enthalpy, $\Delta H = 14$ kJ/mol) and (B) energy indicated by potential functions used for water simulations ($\Delta H = 22$ kJ/mol). C is the critical point. For (A), the phase diagram is consistent in form with that derived from the Haar-Ghallaiger-Kell equation of state (148) and suggests that a liquid-liquid first-order transition with negative Clapeyron slope run between the liquid vapor spinodal at negative pressure and uncharted regions at high pressure. For (B), the line of first-order transitions terminates at a critical point at moderate pressures, marked C'. This result is also obtained in computer simulations with common pair potentials (78). Note the disposition of the spinodal lines above and below the transition line. Approach to a spinodal is accompanied by diverging fluctuations and anomalous physical properties. Dotted lines are loci of temperatures of maximum density. [Adapted from (76) by permission copyright American Institute of Physics]

ized as separate megabasins in the configuration space of a single substance. The megabasins in these cases are separated by major energy barriers such that the system can, under the right circumstances, execute transitions between them that have the characteristics of first-order phase transitions. For instance, this is necessary to account for the polyamorphic transition seen to occur, under nonergodic conditions, in the case of vitreous water described above. Such transitions may occur in the metastable liquid state where, at least in principle, the transition can be a reversible phenomenon.

The microstructure of a quenched melt in the $Y_2O_3-Al_2O_3$ (70) system is shown in Fig. 5. The structure shows droplets of one glass phase embedded in the matrix of another. Such microstructures are seen frequently in quenched oxide glass melts where they arise from the passage of the melt through a submerged (metastable) liquid miscibility gap. The two phases are necessarily, in this case, of different composition. $Y_2O_3-Al_2O_3$, however, is not the type of system in which such a miscibility gap would be expected. Indeed, painstaking analysis showed (70) that the two glassy phases in Fig. 5 are of identical composition. Only the densities are different. The droplet phase, which must have nucleated and grown from the matrix, is the low-density, low-entropy phase. A first-order transition from a high-density to a low-density liquid must have occurred during the quench but was arrested before completion because of the fast quench and the highly viscous conditions under which the nucleation was initiated. The high-temperature liquid, according to the available viscosity data and the best estimate of T_g for the droplet phase, is a very fragile liquid, so it is not unreasonable to suppose that the transition is also one from a fragile to a strong liquid.

This picture is entirely consistent with what had already been suggested (71) for the behavior of pure water during quenches

so rapid that the glassy state is obtained (72). Exceptionally fast cooling is needed as the T_v/T_m ratio for water is only 1.36. Both the thermodynamic and the transport properties of water approaching $-45^\circ C$ become highly anomalous (73) and comparable to those of some liquid crystals approaching their weakly first-order mesophase transitions (74). The anomalies are a consequence of approach to a spinodal instability, near which fluctuations slow down and diverge, that lies just below the first-order transition temperature. The low-temperature phase of water is an open network (75) like SiO_2 , and it is not surprising (Fig. 4) that it should be a strong liquid (71).

The manner in which such weak first-order transitions can arise in atomic and small molecule liquids prone to open network bonding has been demonstrated in two recent theoretical papers (76, 77), one of them a microscopic model (77). The phase diagrams for two water-like substances with different hydrogen bond strengths obtained (76) are shown in Fig. 6 (omitting all crystalline phases). The value of the bond strength determines whether a first-order liquid-liquid transition occurs at all pressures or only at pressures above ambient. Again, the low-temperature phase is a low-density, low-entropy phase.

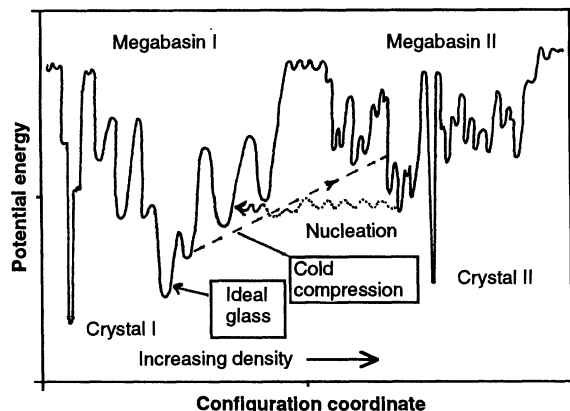
The slopes of the liquid-liquid phase transition lines in Fig. 6 are those expected from the Clapeyron equation and, in combination with the spinodal lines radiating out from the critical point, shows why the polyamorphic phase change observed under nonergodic conditions in both laboratory (8, 9) and simulation studies, (78) occurs hysterically under nonergodic conditions (9, 76, 78). The amorphization of certain high-pressure metallic phases transforming to low-density tetrahedral semiconducting glasses on decompression (79), has been explained by using similar phase diagrams (which have second critical points at negative pressures) derived from "two-fluid" models (80).

A situation analogous to the latter cases exists for two other well-researched amorphous substances which also exhibit tetrahedral coordination in their low energy states, silicon and germanium. A thermodynamic problem in the relation between liquid and amorphous silicon, comparable to that for water (6), was pointed out by Spaepen and Turnbull (81). They proposed as a solution that amorphous silicon should pass into the liquid state *not* continuously as for normal glasses but through a first-order "melting" transition, at a temperature well below the normal T_m . Again, proof was not possible at that time because of the extremely rapid crystallization to the four-coordinated crystal form. However, the advent of laser heating made extremely fast heating possible, and it was subsequently reported by Thompson *et al.* (82) that amorphous silicon "melted" at a temperature of 1480 ± 50 K, which is some 200 K, or 12%, below T_m of the ordered crystal. For water, the proposed transition, also possibly a first-order melting just above a spinodal at 227 K, would occur $\sim 15\%$ below T_m . It is an interesting question whether or not Si, maintained in the amorphous state at 1400 K by, for instance, a crystal-order-destroying beam of electrons, would be an amorphous solid or a viscous liquid. The latter may be more reasonable given that, among known glasses, all except SiO_2 are above their T_g at 1400 K—in which case the "melting" transition reported for Si is actually a liquid-liquid transition. Indeed, such a transition has been observed in computer simulation studies of liquid Si by Grabow (83).

To accommodate these new phenomena, a more general version of the hypersurfaces discussed earlier is presented in Fig. 7. The new version permits the low-entropy "strong" liquid state to be found by a first-order phase change (configuration space tunnelling) from a fragile (higher entropy) state, which involves nucleation and growth as evidenced in Fig. 5. Now, at low temperatures, the possibility of nucleating a phase change, hence observing an equilibrium transition, vanishes but the phase change can still occur by a spinodal-type mechanism. The system can be moved by elastic distortions along a continuous uphill path in the configuration space of one megabasin until an overlap with a minimum in the adjacent megabasin occurs and the system "falls" into it. This path is absolutely irreversible, and the transition on decompression can only be accomplished by a comparably large elastic distortion in the opposite direction—hence, the large hysteresis (84) demonstrated so definitively by Mishima (9) and by Poole *et al.* (78).

The above phenomena can be related to the phase behavior of liquid crystals whose transitions have been analyzed in detail

Fig. 7. Potential energy hypersurface showing megabasins needed to understand the existence of polyamorphic forms, and the observed first-order-like phase transitions between them. The wavy horizontal arrow indicates a narrow channel in configuration space (out of the plane of the paper) by which nucleation of a low-entropy phase can occur during cooling (strictly, the vertical axis should be a chemical potential in order for the horizontal transition to be appropriate). The inclined straight line schematizes how cold compression can lead to sudden (unnucleated, spinodal-like) collapse to a higher density glass. In addition to Stillinger's article (64), see the review of the glassy state (with an emphasis on spin glasses) by Anderson (149).



(70). The only novelty being introduced here is that such phase transitions can occur in systems of small molecules, even atoms, and that they may be responsible for a switch from strong to fragile behavior in the liquid, and for hysteretic pressure-induced first-order phase transitions in the glass. In these new cases, the innate asymmetry of the liquid crystal-forming molecules has been replaced by an innate predisposition to a special low coordination number, short range order—which means these phase transitions are accompanied by larger changes of volume than in the liquid crystal case. The existence of vitreous states of different liquid crystal mesophases has long been known (85). Together with the vitrified native and denatured low moisture proteins that have been used as glues since ancient times, they stand as early unheralded manifestations of the vitreous state polymorphism phenomenon.

Other Canonical Features of Liquids near T_g

The only non-Arrhenius behavior is one of three canonical features of the viscous liquid state. So far liquids have been discussed as having only a single time constant associated with their transport or relaxation processes. The viscosity, of course, is a measure of the liquid response to a suddenly imposed shear stress and is related to the corresponding relaxation time by a Maxwell equation:

$$\eta = G_\infty \tau_s \quad (4)$$

where G_∞ is the high-frequency shear modulus, an elastic property, and τ is the average relaxation time of the system as it responds to the impressed shear stress. In statistical mechanics, it is the integral of the shear stress tensor time auto-correlation function and as such can be evaluated from molecular dynamics calculations. For liquids exhibiting non-Arrhenius relaxation time behavior, this correlation function is not a simple exponential even when the effects of molecular oscillations, which are seen at very short times, have been averaged out. Much attention has been given to the interpretation of this complex departure from exponentiality. What can be said here is that there appears (85–90) to be a correlation between the departures from exponential relaxation and from Arrhenius temperature dependence, that is, with the liquid fragility.

When compared at some fixed relaxation time such as 10^2 s at T_g departure from exponentiality is most conveniently characterized by the stretching exponent β of the Kohlrausch-Williams-Watts relaxation function:

$$\theta(t) = \exp - [(t/\tau)^\beta] \quad (5)$$

which has been shown (91) to give a one-parameter description that is as good as that obtained with the two-parameter Havriliak-Negami equation (92). The correlation, however, is different for liquids of different structural complexity (92); β usually decreases with decreasing temperatures. For spin glasses, some of which are much more fragile than structural glasses (47) and hence can be studied much closer to T_o , the responses are so extremely nonexponential that Eq. 5 is inadequate to describe them. Attempts with Eq. 5 yields $\beta < 0.05$ (82, 83).

It is reasonable to ask how β changes at temperatures below T_g . The provocative answer (87, 93) is that it tends to a limit at T_o of Eq. 2. A scaling analysis of this phenomenon recently lead Menon and Nagel (93) to conclude that the susceptibility itself would diverge at T_o , thereby strongly supporting the underlying phase transition notion to be taken up next.

The third canonical characteristic of relaxing complex liquids is the so-called non-linearity of relaxation (10, 94). This refers to the finding that near and below T_g , relaxation can be studied on systems which are nonergodic and are evolving toward the equilibrium structure on very long time scales. The process is known as “annealing” when it occurs by design, and “aging” when it occurs unwanted. It has been much studied in the glass industry where it is frequently referred to as “stabilization.” In the polymers industry it is known as “aging” and is the focus of the article by Hodge in this issue (95). In the nonergodic state it is usually found that the shorter the (average) relaxation time measured by a particular technique at a constant temperature the greater the nonergodicity (measured in terms of departures of macroscopic properties, such as volume and entropy from their equilibrium values). Hodge (95, 96) found that the more fragile the liquid, the greater is the dependence of the measured relaxation time on this departure from equilibrium. By combining the Adam-Gibbs entropy theory for relaxation (61) and the Tool-Narayanaswamy treatment of out-of-equilibrium relaxation (10, 97, 98), almost quantitative accounts have been given (99, 100) of the glass transition and related phenomena, even including relaxation of vapor-deposited glasses (101).

Thermodynamic Aspects of the Glass Transition

Although this article began with a description of the glass transition phenomenology with a thermodynamic observation (ΔC_p) only kinetic phenomena have been dis-

cussed. Now it is time to return to thermodynamics, because much has been implied but little said.

The higher C_p of the liquid above T_g , for instance, has important consequences. It requires that a new contribution to the enthalpy ΔH and entropy ΔS of the substance begins at T_g . This is clearly the main source of the entropy of fusion ΔS_f because the latter is largely accounted for by the ΔS added between T_g and T_f . Looked at the other way, the decrease in ΔS below T_f would appear to be correlated with the manner in which the liquid “slows down.” This is shown in Fig. 8A, where the ratio of that of the entropy excess S_{ex} of the liquid to that of the crystal at temperatures below T_m is shown [for a collection of molecular and ionic liquids of varying fragility (59)] as a fraction of the entropy of fusion, $\Delta S_f = S_{ex}$ at T_f . A reduced temperature scale is used to simplify the comparisons. CKN is not included because it is a solution. Figure 8B shows how the excess heat capacity ΔC_p increases with decreasing temperature, thereby accelerating the approach to the entropy crisis. In the same range the log-(viscosity) is rocketing up because of its apparent connection to the excess entropy, which we now discuss.

At T_g , the value of $S_{ex}/\Delta S_f$ has typically fallen to 0.4 and in some cases it is diminishing so quickly that it would vanish just 10% below T_g . That the total entropy of the liquid is approaching the crystal value on such a sharp trajectory constitutes an entropy crisis, since a continuation of the trend below T_g would quickly produce a disordered state with entropy much less than that of the stable ordered state, which is not acceptable within conventional thermodynamic thinking. This much-discussed problem was pointed out in a seminal paper by Kauzmann in 1948 (102). It is the primary basis for the idea that the glass transition is at the root of a thermodynamic transition hidden by slow kinetics, because some sudden change in the C_p of the internally equilibrated liquid is needed to avoid the liquid of subcrystalline entropy (103). The extrapolated isoentropy temperature has become known as the Kauzmann temperature T_K .

The idea of a ground state for amorphous packing is contained in the representation of the potential energy hypersurfaces of Fig. 7. The lowest minimum on the surface would be the one that the system would occupy if the cooling process were so slow that the liquid would reach T_K in equilibrium. However, as Fig. 4 and Eq. 1 suggest, this would require infinitely slow cooling. Thus T_K , like absolute zero, is inaccessible.

The rate at which the configurational entropy increases depends on the number of minima per unit of energy increase. Thus the surfaces with the largest densities of minima

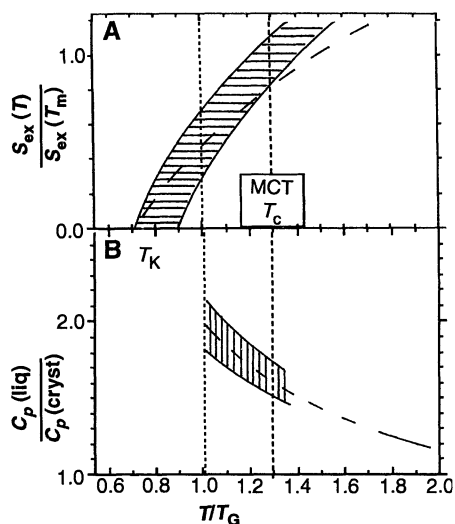


Fig. 8. (A) Decrease of the excess entropy of liquid over crystal from that at the melting point [$S_{\text{ex}}(T_m)$] for nine glass-forming molecular and ionic liquids during supercooling. Temperatures are scaled by T_g so that the difference in excess entropy at T_g is easily seen. Note how rapidly the ratios approach zero at T_g at the right-hand extreme of the band. The dashed vertical lines indicate, respectively, the temperatures T_g defined as in Fig. 2, and T_c , the mode coupling theory critical temperature obtained from viscosity data fitting (59). The dashed curve is the distinct behavior of ethanol, which is intermediate in Fig. 4. The other liquids are all more fragile. (B) Variation of the ratio of liquid-to-crystal heat capacity ratio with temperature for various liquids. The trend is well approximated by a hyperbolic temperature dependence, $\Delta C_p \sim T^{-1}$. The dashed line shows the extended data, interpolated between T_g and T_m , for a metallic glass former, Au-Si [see the article by Greer (150)].

will be those for systems with large ΔC_p and high fragilities. The connection between all of these characteristics is best made through the Adam-Gibbs equation which resulted from a heuristic theory of cooperative relaxation (60). The final equation:

$$\tau = \tau_0 \exp(C/TS_{\text{ex}}) \quad (6)$$

becomes identical with the VTF equation for the case in which the excess heat capacity ΔC_p varies inversely with temperature, which is a fair approximation to the observed behavior seen in Fig. 8. The equation gives a direct explanation of the coincidence of T_K with T_c , which has frequently been found (48, 50, 107–109).

The above is one version of the “view of the glass transition from the liquid,” and MCT provides another. However, there is a quite different view of the glass transition which is a “view from the solid.” In this view (109), one starts knowing nothing about the liquid and asks what is it about the vibrational dynamics of an amorphous solid, formed by any one mechanism that has no liquid state in its history, that causes it suddenly to generate entropy of a new

type, and become diffusive and mobile, when heated at a fixed rate above some special temperature T_g ? This is a legitimate approach which, like the idealized MCT, denies any need to answer questions about what happens on infinite time scales at low temperatures other than the assertion that an entropy-generating mechanism, which works at higher temperatures, has become inoperative. This approach is examined in the last section of this article.

“Glassy” Dynamics and Phase Transitions in Polypeptides and Proteins

The relaxational phenomena that occur in native proteins can be interpreted in terms of so-called “glassy” dynamics (4, 110–119), which usually means the dynamics of glass-forming systems above T_g . These single molecule systems display many of the dynamical features of the many-molecule systems discussed above. An individual protein molecule contains so many individual rearrangeable subunits that its configuration space can be described by a potential energy hypersurface containing most of the features of the hypersurfaces typical of a many-particle glass-forming system. To what extent does the superstructure imposed by the folding of the protein into its native state impede the exercise of the liquidlike degrees of freedom at temperatures below the folding transition? Obviously considerable freedom remains because the protein function involves fast conformational changes.

This question is answered operationally by examining C_p of a concentrated water-in-protein solution (or a dry protein in certain cases) before and after denaturation. Figure 9 shows differential scanning calorimeter scans of a globular protein of variable water content before and after denaturation (117). The denatured system has a quite pronounced glass transition, and the dry native state shows little or none. The thermal effect in the native protein becomes somewhat more pronounced with increasing water content but is never comparable with the denatured sample nor with that of simple polypeptides of comparable molecular weight and water content. This distinction is, in fact, what might be expected for strong and fragile polyamorphs. Is it possible that the unfolding transition in a single protein molecule, which involves the cooperative breaking of many hydrogen bonds, is the initially low-density folded structure (120), generically related to the strong-to-fragile liquid transition in water? Certainly there is a change in mobility of chain links as the transition is crossed (120). Furthermore, Morozov and Morosova (121) give evidence for the existence of a mechanical instability (a spi-

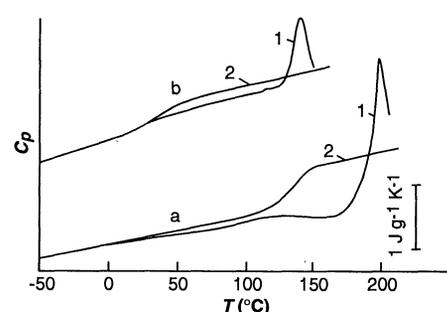


Fig. 9. Differential scanning calorimeter scans of the globular protein legumin both before and after denaturation, for different water contents (A) dry and (B) 10.4% by weight. Note the increase in calorimetric strengths of glass transitions after denaturation. The native state acts like a strong liquid. Comparison of the glass transition with a simple homopolypeptide, poly-L-asparagine is made in Fig. 10. [From (117b) by permission copyright Oxford University Press]

nodal) in the crystal phase lying just above the denaturing transition temperature (as in Fig. 6 for water). They argue that the instability in the crystal is intimately related to the instability in the molecules.

In Fig. 10 the dependence of T_g on water content in (i) denatured proteins, (ii) a native protein of unsubstantial tertiary structure (wheat gluten) (122), and (iii) a polyhomopolypeptide, are compared with data for a classical polymer-diluent system (polystyrene-styrene). Figure 10 shows that denatured proteins are members of the family of lightly plasticized chain polymers. With increasing water content the (high-temperature) denatured protein T_g decreases and loses definition while the native protein phenomenon gains definition (117). At saturation, there is little distinction between them (119) [although what is actually observed at high water contents is more in the nature of a strong secondary relaxation (119)]. It seems reasonable to regard the water-saturated folded protein also as a plasticized polymer system.

The effect of pressure on the denaturing transition studied by different workers, in particular by Zipp and Kauzmann (123) and Markley and co-workers (120) proves to be such that the previously favored hydrophobic model for the folding transition is not supported. In the cases studied by these authors, the volume change of the protein itself on unfolding [much more so than of the protein-in-water system in toto (120)] was found to be strongly negative, in the same sense as (and comparable in magnitude to) the volume change for forming high-temperature water from low-temperature water is negative. The basic ingredients for the bond-modified van der Waals model (76) which give the phase transition in water, are therefore present. Further consideration of the analogy seems warranted.

Anharmonicity, Boson Peaks, and the Glass Transition Viewed from the Solid

A phenomenon frequently termed a transition (implicitly a glass transition) by protein researchers (despite its observation in extremely short-time experiments) is the sudden change of slope occurring in the T -dependence of the Debye-Waller factor, the mean square displacement (MSD) of the system's particles ($\langle r^2 \rangle$). It applies to observations based on Mössbauer scattering, which is very sensitive to small-amplitude displacement (113), and on neutron-scattering studies (114). It has also been seen, with much greater difficulty and less definition, by x-ray studies of protein crystals (115), and with considerable definition in computer simulations of myoglobin (116).

This same phenomenon has now also been found in simple liquids (124) and chain polymers (125–128). In these cases, the observed effect has been attributed to the onset of inelastic processes and has been interpreted (124, 125) in terms of MCT. In a study of the simplest available glass-forming system, selenium, which is also a chain polymer, Buchenau and Zorn (129) gave an alternative interpretation based on the concept of soft phonons. A number of the observations are collected in Fig. 11 (the calorimetric T_g values are noted in the legend of Fig. 11). The proximity of the anomaly to T_g may be seen from the T_g -scaled plot of the data shown in the insert to Fig. 11.

In my group we examine this phenomenon (1, 130) for a range of ionic liquids, from extremely fragile ($\text{BaF}_2 \cdot 2\text{ZrF}_4$) to extremely strong (SiO_2), which can be simulated by using the ion dynamics programs that have been developed for the study of ionic liquids and glasses (131–133). A special advantage of the computer simulation studies is that the phenomenon can be observed within an unchanging configuration because the onset of diffusion which permits the structure to change and evolve in a liquidlike fashion in laboratory studies at $T > T_g$ is eliminated by the short duration of the simulation. The absence of any structural rearrangements of importance to diffusion is proven by the absence of any net slope in the MSD time curve over many hundreds of individual ion oscillations (130).

Systems of variable dimensionality of network connectivity were studied in Fig. 12A. Two of these, SiO_2 and B_2O_3 , correspond to familiar inorganic glass systems. The first is a three-dimensional (3D) network of silicon atoms four-coordinated by oxygen atoms whereas the second has a two-dimensional (2D) structure of O-linked three-coordinated boron atoms with weak interactions between the sheets. The third one, which has a one-dimensional (1D)

character, is a system recently described by Lucas and colleagues (134) and is obtained by substituting F^- for oxide ions in B_2O_3 , such as to dismantle the 2D sheet structure of B_2O_3 into 1D chains $(\text{BOF})_n$. (Special measures have to be taken in the setting up of the initial configuration for this latter system to avoid cross-linking events which are statistically probable in the fused state, although the presence of a limited number of such cross-links has little effect on the behavior. The onset of such crosslinking occurs on heating at ~ 650 K). It therefore resembles the chain polymers of Fig. 11.

Figure 12 shows how $\langle r^2 \rangle$, evaluated between 0.5 and 2.0 ps, varies with T from low T to values well above T_g [see (1) and (130)]. Included in Fig. 12 are the neutron scattering data from Fig. 11. The similarity of the Se behavior to that of our 1D BOF system is impressive and would be greater if Se did not change its configuration with time for $T > T_g$. Comparison of Figs. 11 and 12 suggests that the breaks in the Debye-Waller factor referred to earlier for both biological and other systems owe their origin to the onset of severe anharmonicity in the molecular-ionic motions, rather than to the presence of inelastic processes as argued

in (125, 126). However, the two views can be reconciled by recognizing (135) that the overshoot in $\langle r^2 \rangle$ seen at 0.1 to 1.0 ps (particularly persistent for B_2O_3 and SiO_2) is a time-domain manifestation of the much-discussed boson peak (125, 127, 129, 135–141). Damping of this overshoot appears as the inelastic process detected by neutron scattering and is largely responsible for increased $\langle r^2 \rangle$ above T_g . Damping occurs below T_g for the 1D system [also in the fragile $\text{BaF}_2 \cdot \text{ZrF}_4$ case (130)] but only far above it for B_2O_3 (2D) and SiO_2 (3D), in accord with the observation (138) that the boson peak persists above T_g in strong liquids.

The only laboratory system for which the incoherent neutron scattering data have been presented in the $\langle r^2 \rangle$ versus time form is that of polyvinyl chloride (141). This is the most fragile liquid known (46) and, since the boson peak disappears below T_g in fragile liquids (138), the overshoot in $\langle r^2 \rangle$ is barely observable at any of the temperatures studied. An $\langle r^2 \rangle$ versus time presentation of experimental incoherent neutron scattering data for the cases of B_2O_3 or SiO_2 would probably be informative. The overshoot in $\langle r^2 \rangle$ is a particularly striking feature in the case of B_2O_3 , for which also a

Fig. 10. Glass transition temperatures for various biopolymers and polystyrene as function of water (or other molecular additive) content, showing the similarity of denatured protein behavior with that of other chain polymer plus diluent systems. Insert shows type of scans on which individual points are based: the scan of the poly-L-asparagine sample with 14% H_2O by weight (solid line) shows a sharper glass transition than the scans of denatured legumin (6% H_2O , dotted line) and collagen (10% H_2O , dashed line). [From (132) by permission copyright American Institute of Physics]

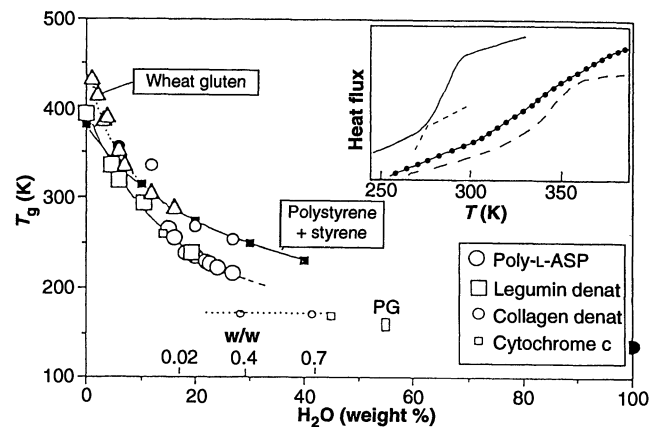
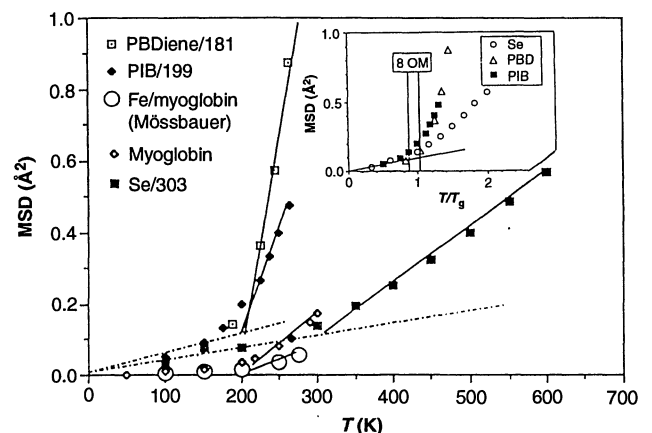


Fig. 11. Variations of the Debye-Waller factor, $\langle r^2 \rangle$ with T_g -scaled temperature, showing change of slope around the temperature of the calorimetric glass transition, T_g . T_g values in Kelvin degrees are given in legend; PBDiene, polybutadiene, and PIB, polyisobutylene. Insert shows the same data versus T/T_g , except for proteins for which T_g is only ambiguously defined by calorimetry. The band marked 8 OM shows the reduced temperature range needed to change the relaxation time of a fragile liquid, *o*-terphenyl, by eight orders of magnitude.



very strong boson peak has been reported (140). This strong effect may be related to concerted motions of ions in the 2D sheet structure of B_2O_3 glass. In this case, the effects should diminish rapidly with addition of alkali oxide, or with application of pressure, both of which promote four-coordination of boron. Indeed, a systematic variation of the correlation length for the intermediate range order with alkali oxide content in the binary system has recently been demonstrated (140). For SiO_2 , the overshoot at higher temperatures is quickly damped out by increasing pressure (130).

Breaks in the $\langle r^2 \rangle$ versus T plots of stimulated systems [Fig. 12 and (130)] all seem to occur close to the temperatures of the experimental T_g , as was previously observed in laboratory experiments on elemental selenium (128). However, T_g is defined in a quite arbitrary manner on the basis of measurements conducted at a convenient laboratory time scale, and corresponds, as noted earlier, to a structural relaxation time of 10^2 . While it is simple to say that the structural rearrangement process observed in the laboratory studies could not occur on any time scale without the presence of anharmonicity in the vibrational motions, this does not explain why its onset temperature should seem to be close to the temperature at which the relaxation time happens to be 10^2 s.

This apparent problem is largely re-

solved by recognizing how narrow is the range of T (as opposed to $1/T$) over which the relaxation time changes from small to very large values. We have marked (as 8 OM) on the temperature axis of Fig. 11, the range of temperatures over which the relaxation time changes by eight orders of magnitude from 10^{-4} s to 10^{+4} s for a typical fragile liquid. It is seen to be a narrow interval relative to the total T range explored. This is a consequence of the very high-temperature coefficient of the relaxation time in the vicinity of T_g for fragile liquids, in accord with Eq. 2 with small D . For strong liquids, the T range for the same change of relaxation time is greatly extended but then, also, the discontinuity between the harmonic and anharmonic ranges is much less well-defined, presumably because of the persistence of the boson peak above T_g . [In Ngai's model (142) this would correspond to the primitive relaxation having a very large activation energy, and in Harrowell's development of the 2-spin facilitated Ising model (137, 143) it would correspond to the spin flip process having a large activation energy.]

The short time phenomenon, which has been thought of as a glass transition in protein dynamics experiments (110–115) and protein computer simulation studies (116), can be viewed as a precursor or trigger phenomenon to the real glass transition. It is also evidently (142) the primitive relaxation of Ngai's coupling model, seen in a somewhat different light. The real glass transition, characterized by the C_p jump, depends on diffusive displacements that only occur on very much longer time scales. A possible connection is that made by Buchenau and Zorn (129), who outlined a critical displacement model in analogy to the Cohen-Turnbull "critical free volume model" for diffusion in glass-forming simple liquids (144). The ΔC_p associated with the anomalous Debye-Waller effect, which now seems to be intimately related to the overdamping of the boson peak, can be measured in computer simulation studies and seems to be small (130). If the overdamping of the boson peak really triggers the glass transition, then the more anharmonic are the vibrations associated with this peak (that is, with the intermediate range order or structural inhomogeneities) the lower in temperature (hence the closer to T_K) the configuration space exploration should begin (at T_g). Because T_g/T_K scales with the liquid strength parameter (D in Eq. 2), the fragility should then be determined by the anharmonicity as implied in (138). Large anharmonicity means large volume dependence of the important frequencies (the Gruneisen parameter) hence presumably implies high pressure coefficients of T_g , as are indeed found for fragile liquids (145).

Proteins, in terms of the above considerations, seem to be both strong and fragile because they show a sharp change in $\langle r^2 \rangle$ versus T at ~ 200 K (113, 114) yet have a boson peak that persists far above 200 K (146). The resolution of this paradox is probably to be found (119) in the separation of protein dynamics into β -like components due to water-to-side chain interactions (mainly on the surface) which become active at 170 K, and strong α -like components associated with main chain motions that are responsible for the persistent boson peak at much higher temperatures. Little information on the behavior of the boson peak in proteins after denaturation is available, and what is available seems conflicting (146).

Concluding Remarks

The field of viscous liquids and the glass transition has certainly been enriched by recent developments and offers more challenges than ever before. Key problems include:

1) Determining the conditions under which polymorphism is or is not manifested, and contrasting the physical properties of the two viscous liquid states.

2) Determining the general behavior of liquids near their T_g at high pressure (147), where attractive forces will be less important.

3) Understanding the structural origin of the boson peak, the nature of its damping, and the significance of anharmonicity in general.

REFERENCES AND NOTES

1. C. A. Angell, P. H. Poole, J. Shao, *Nuovo Cimento*, in press.
2. D. R. Uhlmann, J. F. Hayes, D. Turnbull, *Phys. Chem. Glasses* **8**, 1 (1967).
3. E. J. Sare, thesis, Purdue University, West Lafayette, IN (1970).
4. I. E. T. Iben *et al.*, *Phys. Rev. Lett.* **62**, 1916 (1989).
5. L. Slade, H. Levine, J. W. Finley, in *Protein Quality and Effects of Processing*, R. D. Phillips and J. W. Finley, Eds. (Dekker, New York, 1989).
6. C. A. Angell and E. J. Sare, *J. Chem. Phys.* **52**, 1058 (1970).
7. The term "polymorphism" was suggested by Wolf, whose studies on pressure-induced amorphization mechanisms in FeO_2 have been the most thorough in the field; G. H. Wolf *et al.*, in *High-Pressure Research: Application to Earth and Planetary Sciences*, Y. S. Manghnani and M. H. Manghnani (American Geophysical Union, Washington, DC, 1992), pp. 503–517.
8. D. Mishima, L. D. Calvert, E. Whalley, *Nature* **310**, 393 (1984); *ibid.* **314**, 76 (1985); G. Mishima, K. Takemure, K. Aoki, *Science* **254**, 406 (1991).
9. O. Mishima, *J. Chem. Phys.* **100**, 5910 (1994).
10. C. T. Moynihan *et al.*, *Ann. N.Y. Acad. Sci.* **279**, 15 (1976).
11. L. M. Torell and C. A. Angell, *J. Chem. Phys.* **78**, 937 (1983).
12. R. Palmer and D. L. Stein, in *Relaxations in Complex Systems*, K. Ngai and G. B. Wright, Eds. (National Technical Information Service, U.S. Department of Commerce, Springfield, VA, 1984), p. 253.
13. The MCT introduced by W. Götze and collaborators

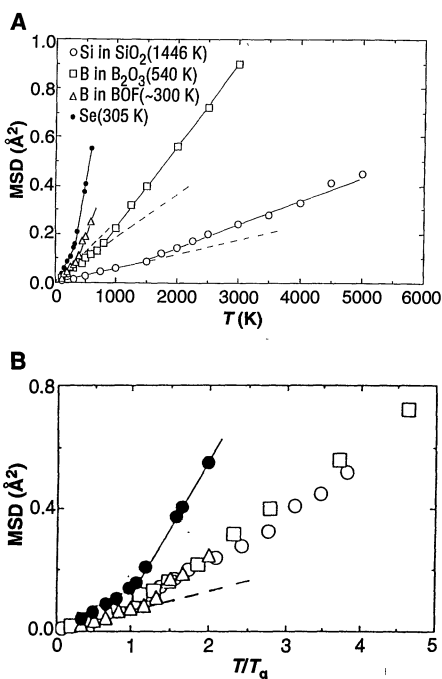


Fig. 12. (A) Variations of $\langle r^2 \rangle$, in the prediffusion regime with temperature for computer-simulated SiO_2 (3D network), B_2O_3 (2D sheet), and BOF (linear chains). T_g values are given in parentheses. Included are laboratory neutron scattering data from (137) for the case of selenium, which has T_g close to that of BOF. (B) Same data versus T/T_g , where T_g is the calorimetric T_g .

- in the 1980s has been the most influential development in glass science since the development and interpretation of semiconducting and switching glasses.
14. U. Bengtzelius, W. Göetze, A. Sjölander, *J. Chem. Phys.* **17**, 5915 (1984).
 15. W. Göetze, in *Liquids, Freezing, and the Glass Transition*, J. P. Hansen and D. Levesque (Plenum, New York, 1989); W. Göetze and L. Sjögren, *Rep. Prog. Phys.* **55**, 55 (1992).
 16. A. Dietzel and H. J. Poegel, in *Proceedings III International Congress on Glass*, A. Garzanti, Ed. (Nello Stabilimento Grafico Di Roma Della, Rome, 1954), p. 219.
 17. C. A. Angell, *J. Non-Cryst. Solids* **131-133**, 13 (1991).
 18. P. Harrowell, *Phys. Rev. E* **48**, 4359 (1993).
 19. R. V. Chamberlin, *J. Non-Cryst. Solids* **172-174**, 318 (1994).
 20. K. Schmidt-Rohr and H. W. Spiess, *Phys. Rev. Lett.* **66**, 3020 (1991).
 21. C. T. Moynihan and J. Schroeder, *ibid.* **160**, 52 (1993).
 22. B. Geil and G. Hinze, *Chem. Phys. Lett.* **216**, 51 (1993).
 23. C. A. Angell, J. H. R. Clarke, L. V. Woodcock, *Adv. Chem. Phys.* **48**, 397 (1981).
 24. J. H. R. Clarke, *J. Chem. Soc. Faraday Trans. II*, **75**, 1371 (1979).
 25. J. R. Fox and H. C. Andersen, *Ann. N.Y. Acad. Sci.* **371**, 123 (1981); *J. Phys. Chem.* **88**, 4019 (1984).
 26. This fortunate but predictable circumstance makes feasible the testing of fundamental theories for behavior of supercooled liquids on the idealized systems for which the theories are usually constructed.
 27. C. A. Angell and Y. Choi, *J. Microsc.* **141**, 251 (1986).
 28. W. B. Hillig and D. Turnbull, *J. Chem. Phys.* **24**, 914 (1956); D. Turnbull, *Contemp. Phys.* **10**, 473 (1969).
 29. D. R. Uhlmann, *J. Non-Cryst. Solids* **7**, 337 (1972).
 30. P. F. James, *Phys. Chem. Glasses* **15**, 95 (1974); G. F. Neilson and M. Weinberg, *J. Non-Cryst. Solids* **34**, 137 (1979).
 31. P. F. James, in *Nucleation and Crystallization in Glasses*, vol. 4 of *Advances in Ceramics*, J. H. Simmons, D. R. Uhlmann, G. H. Beall, Eds. (American Ceramic Society, Columbus, OH, 1982).
 32. D. R. MacFarlane, R. K. Kadiyala, C. A. Angell, *J. Phys. Chem.* **87**, 1094 (1983); H. Senapati, K. K. Kadiyala, C. A. Angell, *ibid.* **95**, 7050 (1991).
 33. D. Turnbull and M. H. Cohen, *J. Chem. Phys.* **29**, 1049 (1958).
 34. C. A. Angell, A. Dworkin, P. Figuiere, A. Fuchs, H. Szwarc, *J. Chim. Phys.* **82**, 773 (1985).
 35. These are based on the applicability of certain thermodynamic relations between the transition temperature and the jumps in heat capacity and expansion coefficient appropriate to second-order transitions which are found to apply at the glass transition and on the Kauzmann entropy paradox discussed in a later section.
 36. C. A. Angell, in *Relaxations in Complex Systems*, K. Ngai and G. B. Wright, Eds. (National Technical Information Service, U.S. Department of Commerce, Springfield, VA, 1985), p. 1.
 37. H. Vogel, *Z. Phys.* **22**, 645 (1921).
 38. G. S. Fulcher, *J. Am. Ceram. Soc.* **8**, 339 (1925).
 39. G. Tammann and W. Z. Hesse, *Anorg. Allgem. Chem.* **156**, 245 (1926).
 40. Neither Vogel (37) or Fulcher (38) who first utilized Eq. 1 to describe liquid viscosities, paid any attention to its physical significance whereas Tammann, the vitrearch of the 1930s, who independently developed the equation just 1 year later (39), gave it a detailed and basically correct interpretation. This is why the present author idiosyncratically initiated the use of the latter author's initial in second place in the often cited abbreviation "VTF" equation. The history of the equation is reviewed by Scherer (41).
 41. G. W. Scherer, *J. Am. Ceram. Soc.* **75**, 1060 (1992).
 42. Note that the factor $\log \eta_g/\eta_0$ in Eq. 2 is simply the number of orders of magnitude in the transport variable between the reference temperature T_g and the high-temperature limit as $T \rightarrow \infty$, 17 according to Fig. 4. While it seems never to have been noted, this is the origin of the "universal" parameter C_1 ($C_1 = 17.5$) in the famous empirical Williams Landel and Ferry equation for polymer viscosity temperature dependence. This is easily shown (43) by algebraic manipulation using the mathematical identity of the VTF and WLF equations first demonstrated by Miller (44).
 43. C. A. Angell, unpublished results.
 44. A. A. Miller, *Macromolecules* **11**, 859 (1978).
 45. C. A. Angell, L. Monnerie, L. M. Torell, *Symp. Mater. Res. Soc.* **215**, 3 (1991).
 46. D. J. Plazek and K. L. Ngai, *Macromolecules* **24**, 1222 (1991).
 47. J. Souletie, *J. Phys. (Paris)* **51**, 883 (1990).
 48. C. A. Angell and D. L. Smith, *J. Phys. Chem.* **86**, 3845 (1982).
 49. F. Stickel, E. W. Fischer, A. Schönhals, *Phys. Rev. Lett.* **73**, 2936 (1991); F. Stickel and E. W. Fischer, unpublished results.
 50. P. Dixon, *Phys. Rev. B* **42**, 8179 (1990).
 51. C. A. Angell, L. Boehm, M. Oguni, D. L. Smith, *J. Mol. Liq.* **56**, 275 (1993); A. Schönhals, F. Kremer, A. Hofmann, E. W. Fischer, *Physica A* **201**, 263 (1993).
 52. C. A. Angell and K. J. Rao, *J. Chem. Phys.* **57**, 470 (1972).
 53. W. Kob and H. C. Andersen, *Phys. Rev. Lett.* **73**, 1376 (1984); W. Kob, private communication.
 54. W. M. Du, G. Li, H. Z. Cummins, *Phys. Rev. B*, **49**, 2192 (1994).
 55. G. P. Johari and M. Goldstein, *J. Chem. Phys.* **53**, 2872 (1970).
 56. I. Prigogine and R. Defay, *Chemical Thermodynamics* (Longmans, Green, London, 1954).
 57. R. O. Davies and G. O. Jones, *J. Adv. Phys.* **2**, 370 (1953).
 58. A. V. Lesikar and C. T. Moynihan, *J. Chem. Phys.* **72**, 6422 (1980); *ibid.* **73**, 1932 (1980).
 59. C. A. Angell, *J. Phys. Chem. Sol.* **49**, 863 (1988).
 60. M. Goldstein, *J. Chem. Phys.* **51**, 3728 (1969).
 61. F. H. Stillinger, *Science* **267**, 1935 (1995).
 62. G. Adams and J. H. Gibbs, *J. Chem. Phys.* **43**, 139 (1965).
 63. R. Böhmer and C. A. Angell, *Disorder Effects on Relaxational Processes*, A. Blumen and R. Richert, Eds. (Springer-Verlag, Berlin, 1993).
 64. F. H. Stillinger and T. A. Weber, *Science* **228**, 983 (1984); R. A. LaViolette and F. H. Stillinger, *Phys. Rev. B*, **35**, 5446 (1987).
 65. L. V. Woodcock, C. A. Angell, P. A. Cheeseman, *J. Chem. Phys.* **65**, 1565 (1976).
 66. C. A. Angell, P. A. Cheeseman, C. C. Phifer, *Mater. Res. Soc. Symp. Proc.* **63**, 85 (1986).
 67. P. Vashishta, R. K. Kalia, J. P. Rino, I. Ebbsjö, *Phys. Rev. B* **41**, 12197 (1990).
 68. C. A. Scamehorn, P. H. Poole, C. A. Angell, unpublished results.
 69. S. A. Brawer and M. J. Weber, *J. Non-Cryst. Solids* **38** and **39**, 9 (1980); S. A. Brawer, *Relaxation in Viscous Liquids* (American Ceramic Society, Columbus, OH, 1985).
 70. S. Aasland and P. F. McMillan, *Nature* **369**, 633 (1994).
 71. C. A. Angell, *J. Phys. Chem.* **97**, 6339 (1993).
 72. E. J. Mayer, *J. Appl. Phys.* **58**, 663 (1985).
 73. R. J. Speedy and C. A. Angell, *J. Chem. Phys.* **65**, 851 (1976); C. A. Angell, *Annu. Rev. Phys. Chem.* **34**, 593 (1983).
 74. P.-G. deGennes and J. Prost, *The Physics of Liquid Crystals* (Oxford Univ. Press, Oxford, 1993).
 75. A. H. Narten, C. G. Venkatesh, J. A. Rice, *J. Chem. Phys.* **64**, 1106 (1976); S. A. Rice and M. G. Sceats, in *Water: A Comprehensive Treatise*, F. Franks, Ed. (Plenum, New York, 1982), vol. 7, pp. 83-211.
 76. C. H. Poole, F. Sciortino, T. Grande, H. E. Stanley, C. A. Angell, *Phys. Rev. Lett.* **73**, 1632 (1994).
 77. S. Borrick, S. Sastry, P. Debenedetti, *J. Phys. Chem.* **99**, 3781 (1995).
 78. P. H. Poole, F. Sciortino, U. Essmann, H. E. Stanley, *Nature* **360**, 324 (1992); *Phys. Rev. E*, **48**, 4605 (1993).
 79. V. M. Glazov, S. N. Chizhevskaya, S. B. Evgen'ev, *Russ. J. Phys. Chem.* **43**, 201 (1969).
 80. E. G. Ponyatovsky and O. I. Barkalov, *Meter. Sci. Rep.* **8**, 147 (1992).
 81. F. Spaepen and D. Turnbull, *AIP Conf. Proc.* **50**, 73 (1979).
 82. M. O. Thompson, G. J. Galvin, J. W. Mayer, *Phys. Rev. Lett.* **52**, 2360 (1984).
 83. M. Grabow, private communication.
 84. Through this mechanism changes in structure, hence density, may occur in large thicknesses of amorphous ice such as may be found on some cold celestial bodies. Furthermore, such changes, once they occurred, would be locked in.
 85. G. P. Johari, G. E. Johnson, J. W. Goodby, *Nature* **297**, 315 (1982); G. P. Johari, *Philos. Mag.* **46**, 549 (1982); Russian workers from ISF.
 86. T. A. Litovitz and G. McDuffie, *J. Chem. Phys.* **39**, 729 (1963); K. L. Ngai, R. W. Rendell, Rajagopal, S. Teltler, *Ann. N.Y. Acad. Sci.* **484**, 150 (1986); and many papers in the conference proceedings volumes of *J. Non-Cryst. Solids* **131-133** (1991); *ibid.* **172-174** (1994).
 87. P. Dixon and S. Nagel, *Phys. Rev. Lett.* **65**, 1108 (1990).
 88. R. Böhmer and C. A. Angell, *Phys. Rev. B* **45**, 10091 (1992).
 89. K. L. Nagai, R. W. Rendell, D. J. Plazek, *J. Chem. Phys.* **94**, 3018 (1991).
 90. R. Böhmer, K. L. Ngai, C. A. Angell, D. J. Plazek, *ibid.* **99**, 4201 (1993).
 91. F. Alvarez, A. Allegría, J. Colmenero, *Phys. Rev. B* **47**, 125 (1993).
 92. S. Havriliak and S. Negami, *Polymer* **8**, 161 (1967).
 93. N. Menon and S. R. Nagel, *Phys. Rev. Lett.* **74**, 1230 (1994).
 94. C. T. Moynihan, S. N. Chrichton, S. M. Opalka, *J. Non-Cryst. Solids* **131-133**, 420 (1991).
 95. I. M. Hodge, *Science* **267**, 1945 (1995).
 96. ———, *J. Non-Cryst. Solids* **131-133**, 435 (1991); *ibid.* **169**, 211 (1994).
 97. A. Q. Tool, *J. Am. Ceram. Soc.* **29**, 240 (1946).
 98. O. S. Narayanaswamy, *J. Am. Ceram. Soc.* **54**, 491 (1971).
 99. G. W. Scherer, *ibid.* **67**, 504 (1984).
 100. I. M. Hodge, *Macromolecules* **20**, 2897 (1987).
 101. K. Takeda, O. Yamamuro, M. Oguni, H. Suga, *J. Phys. Chem.*, in press.
 102. A. W. Kauzmann, *Chem. Rev.* **43**, 219 (1948).
 103. This idea is supported by the finding that one of the relations analogous to the Ehrenfest equations of second-order transition thermodynamics:

$$dT_g/dP = VT\Delta\alpha/\Delta C_p$$
 (where $\Delta\alpha$ is the change in expansion coefficient) is nearly always obeyed at the glass transition although the other:

$$dT_g/dP = \Delta\kappa/\Delta\alpha$$
 is not, except in computer glass transitions: The first can be shown to be valid provided the excess entropy is the same when the glass transition commences, irrespective of the pressure (58, 104-106). It is the combination of these two equations which gives the Prigogine-Defay ratio $VT\Delta\alpha^2/\Delta\kappa\Delta C_p$ (56). This ratio is unity for true second-order thermodynamic transitions, and also ergodic-nonergodic transitions in systems in which only one order parameter is needed in addition to T and P to define the state of the system. While this appears to hold true for computer glasses (24), it has never been found to hold for any laboratory glass (10, 58, 106). For these $\Delta\kappa$ always appears to be too large. The failure of the second equation is strong evidence against (102, 104) free volume theories of viscous slowdown which nevertheless continue to be popular among polymer scientists—a tribute to the strength of Flory's influence in this area.
 104. M. Goldstein, *J. Phys. Chem.* **77**, 667 (1973).
 105. T. Moynihan and P. Gupta, *J. Non-Cryst. Solids* **29**, 143 (1987).
 106. J. Jäckle, *Rep. Prog. Phys.* **49**, 171 (1986).
 107. C. A. Angell and K. J. Rao, *J. Chem. Phys.* **57**, 470 (1972); C. A. Angell, *Ann. N.Y. Acad. Sci.* **279**, 53 (1976).
 108. C. A. Angell, L. Boehm, M. Oguni, D. L. Smith, *J. Mol. Liq.* **56**, 275 (1993).
 109. C. A. Angell, *J. Am. Ceram. Soc.* **51**, 117 (1968); R.

- Hall and P. G. Wolynes, *J. Chem. Phys.* **86**, 2943 (1987).
110. H. Frauenfelder, S. G. Sligar, P. C. Wolynes, *Science* **254**, 1598 (1991).
111. W. Doster, A. Bachleitner, R. Dunau, M. Hiebi, E. Lüscher, *Biophys. J.* **50**, 213 (1986).
112. V. I. Goldanskii, Yu. F. Krupyanski, V. N. Fleurov, *Dok. Akad. Nauk SSSR* **272**, 978 (1983).
113. F. Parak, J. Heidemeier, G. U. Nienhaus, *Hyperfine Interactions* **40**, 147 (1988).
114. W. Doster, S. Cusack, W. Petry, *Nature* **337**, 754 (1989).
115. B. F. Rasmussen, A. M. Stock, D. Ringe, G. A. Petsko, *ibid.* **357**, 423 (1992).
116. K. Kuczera, J. Smith, M. Karplus, *Proc. Natl. Acad. Sci. U.S.A.* **87**, 1601 (1990).
- 117a.I. V. Sochava, G. I. Tseretoli, O. I. Smirnova, *Biofizika*, 36 (1991).
- 117b.I. V. Sochava and O. I. Smirnova, *Food Hydrocolloids* **6**, 513 (1993).
118. G. Sartor, A. Hallbrucker, K. Hofer, E. Mayer, *J. Phys. Chem.* **96**, 5133 (1992); G. Sartor, E. Mayer, G. P. Johari, *Biophys. J.* **66**, 249 (1994).
119. J. L. Green, J. Fan, C. A. Angell, *J. Phys. Chem.* **98**, 13780 (1994).
120. K. E. Prehoda and J. L. Markley, in *High Pressure Effects in Molecular Biophysics and Enzymology*, J. L. Markley, C. A. Royer, D. Northrop, Eds. (Oxford Univ. Press, New York, in press), any references cited therein, and J. L. Markley, private communication. Note the important reassessment of packing efficiencies of folded and unfolded states which is made in this study. While the unfolding transition may, like the melting of a small crystal, be a transition between two global minima for the individual molecules, the phenomenon observed in a protein solution is the consequence of this event for very many such molecules, and this has the character of a high positive entropy change, small (net) negative volume change, chemical conversion process.
121. V. N. Morozov and T. Ya. Morozova, *J. Biomol. Struct. Dyn.* **11**, 459 (1993).
122. R. C. Hoseney, K. Zeleznak, C. S. Lai, *Cereal Chem.* **63**, 285 (1986).
123. A. Zipp and W. Kauzmann, *Biochemistry* **12**, 4217 (1973).
124. A. Petry *et al.*, *Phys. B. Condens. Mater.* **83**, 175 (1991).
125. B. Frick and D. Richter, *Phys. Rev. B* **47**, 14795 (1993).
126. B. Frick, D. Richter, W. Petry, U. Buchenau, *Z. Phys.* **B70**, 73 (1988).
127. A. Chahid, A. Alegria, J. Colmenero, *Macromolecules* **27**, 3282 (1994).
128. B. Frick and D. Richter, *Science* **267**, 1939 (1995).
129. U. Buchenau and R. Zorn, *Europhys. Lett.* **18**, 523 (1992).
130. J. Shao and C. A. Angell, unpublished results.
131. L. V. Woodcock, *Chem. Phys. Lett.* **10**, 257 (1971).
132. A. Rahman, R. H. Fowler, A. H. Narten, *J. Chem. Phys.* **57**, 3010 (1972).
133. J. Kieffer and C. A. Angell, *J. Non-Cryst. Solids* **106**, 336 (1988), and other references cited therein.
134. C. Boussard, G. Fontaneau, J. Lucas, *J. Non-Cryst. Solids*, in press.
135. R. J. Roe, *J. Chem. Phys.* **100**, 1612 (1994).
136. A. J. Martin and W. Brenig, *Phys. Status Solidi* **64**, 163 (1974).
137. E. Duval *et al.*, *Phys. Rev. Lett.* **56**, 2052 (1986); A. Boukeneter *et al.*, *ibid.* **57**, 2391 (1986); E. Duval *et al.*, *J. Phys. Condens. Mater.* **2**, 10227 (1990).
138. V. N. Novikov and A. P. Sokolov, *Solid State Commun.* **77**, 243 (1991); A. P. Sokolov, A. Kislink, M. Soltwisch, D. Quitmann, *Phys. Rev. Lett.* **69**, 1540 (1992).
139. L. Börjesson, A. K. Hassan, J. Swenson, L. M. Torell, *Phys. Rev. Lett.* **70**, 4027 (1993).
140. A. K. Hassan, L. Börjesson, L. M. Torell, *J. Non-Cryst. Solids* **172-174**, 154 (1994).
141. J. Colmenero, A. Arbe, A. Alegria, *Phys. Rev. Lett.* **71**, 2603 (1993).
142. K.-L. Ngai, *J. Chem. Phys.* **98**, 7588 (1993).
143. ———, in *Diffusion in Amorphous Solids*, H. Jain and D. Gupta, Eds. (The Minerals, Metals, and Materials Society, Warrendale, PA, 1994), p. 17.
144. M. H. Cohen and D. Turnbull, *J. Chem. Phys.* **34**, 120 (1960).
144. P. Harrowell, private communication.
145. T. Atake and C. A. Angell, *J. Phys. Chem.* **83**, 3218 (1979).
146. S. Cusack and W. Doster, *Biophys. J.* **58**, 243 (1990).
147. C. Herbst *et al.*, *J. Non-Cryst. Solids* **172-174**, 265 (1994).
148. L. Haar, J. Gallagher, G. Kell, G.S. National Bureau of Standards-National Research Council Steam Tables (McGraw-Hill, New York, 1985).
149. P. W. Anderson, in *Ill-Condensed Matter*, R. Ballian, R. Maynard, G. Toulouse, Eds. (North-Holland, Amsterdam, 1979), pp. 161-261.
150. A. L. Greer, *Science* **267**, 1947 (1995).
151. I would like to acknowledge the support of the NSF-DMR under Solid State Chemistry grant DMR9108028-002, and the help of many colleagues through stimulating discussions of this subject area. In particular, I am grateful to U. Buchenau, H. Frauenfelder, T. Grande, W. Kauzmann, W. Kob, P. Madden, J. Markley, P. McMillan, P. Poole, H. Sillescu, F. Sciortino, and G. Wolf.

A Topographic View of Supercooled Liquids and Glass Formation

Frank H. Stillinger

Various static and dynamic phenomena displayed by glass-forming liquids, particularly those near the so-called "fragile" limit, emerge as manifestations of the multidimensional complex topography of the collective potential energy function. These include non-Arrhenius viscosity and relaxation times, bifurcation between the α - and β -relaxation processes, and a breakdown of the Stokes-Einstein relation for self-diffusion. This multidimensional viewpoint also produces an extension of the venerable Lindemann melting criterion and provides a critical evaluation of the popular "ideal glass state" concept.

Methods for preparing amorphous solids include a wide range of techniques. One of the most prominent, both historically and in current practice, involves cooling a viscous liquid below its thermodynamic freezing point, through a metastable supercooled regime, and finally below a "glass transition" temperature T_g . A qualitative understanding, at the molecular level, has long been available for materials produced by this latter preparative sequence; however, many key aspects of a detailed quantitative description are still missing. For-

tunately, focused and complimentary efforts in experiment, numerical simulation, and analytical theory currently are filling the gaps.

The present article sets forth a descriptive viewpoint that is particularly useful for discussing liquids and the glasses that can be formed from them, although in principle it applies to all condensed phases. Conceptual precursors to this viewpoint can be found throughout the scientific literature (1), but most notably in the work of Goldstein (2). The objective here is to classify and unify at least some of the many static and kinetic phenomena associated with the glass transition.

Interaction Potentials

Condensed phases, whether liquid, glassy, or crystalline, owe their existence and measurable properties to the interactions between the constituent particles: atoms, ions, or molecules. These interactions are comprised in a potential energy function $\Phi(\mathbf{r}_1 \cdots \mathbf{r}_N)$ that depends on the spatial location \mathbf{r}_i for each of those particles. The potential energy includes (as circumstances require) contributions from electrostatic multipoles and polarization effects, covalency and hydrogen bonding, short-range electron-cloud-overlap repulsions and longer range dispersion attractions, and intramolecular force fields. Obviously, the chemical characteristics of any substance of interest would substantially influence the details of Φ . Time evolution of the multi-particle system is controlled by the interactions, and for most applications of concern here the classical Newtonian equations of motion (incorporating forces specified by Φ) provide an adequate description of the particle dynamics.

In order to understand basic phenomena related to supercooling and glass formation, it is useful to adopt a "topographic" view of Φ . By analogy to topographic maps of the Earth's features, we can imagine a multidimensional topographic map showing the "elevation" Φ at any "location" $\mathbf{R} \equiv (\mathbf{r}_1 \cdots \mathbf{r}_N)$ in the configuration space of the N particle system. This simple change in perspective from conventional

The author is at AT&T Bell Laboratories, Murray Hill, NJ 07974, USA.